Creating Cross-Linked Lamellar Block Copolymer Supporting Layers for Biomimetic Membranes

Chao Lang[a,b], Yue-xiao Shen[a], Jacob A. LaNasa[b], Dan Ye[a], Woochul Song[a], Tawanda J. Zimudzi[b], Michael A. Hickner[b,e], Enrique D. Gomez[a,e], Esther W. Gomez[a,c], Manish Kumar*[,a,c,d,e], Robert J. Hickey*[,b,e]

[a] Department of Chemical Engineering, [b] Department of Materials Science & Engineering [c] Department of Biomedical Engineering, [d] Department of Civil and Environmental Engineering, [e] Materials Research Institute, The Pennsylvania State University, University Park, PA, 16802 USA

*To whom correspondence should be addressed. Robert J. Hickey rjh64@psu.edu,

Manish Kumar manish.kumar@psu.edu

Abstract

The long-standing goal in membrane development is creating materials with superior transport properties, including both high flux and high selectivity. These properties are common in biological membranes, and thus mimicking nature is a promising strategy towards improved membrane design. In previous studies, we have shown that artificial water channels can have excellent water transport abilities that are comparable to biological water channel proteins, aquaporins. In this study, we propose a strategy for incorporation of artificial channels that mimic biological channels into stable polymeric membranes. Specifically, we synthesized an amphiphilic triblock copolymer, poly(isoprene)-*block*-poly(ethylene oxide)-*block*-poly(isoprene), which is a high molecular weight synthetic analog of naturally occurring lipids in terms of its self-assembled structure. This polymer was used to build stacked membranes composed of self-assembled lamellae. The resulting membranes resemble layers of natural lipid bilayers in living systems, but with superior mechanical properties suitable for real-world applications. The procedures used to synthesize the triblock copolymer resulted in membranes with increased stability due to the crosslinkability of the hydrophobic domains. Furthermore, the introduction of bridging hydrophilic domains leads to the preservation of the stacked membrane structure when the membrane is in contact with water, something that is challenging for diblock lamellae that tend to swell, and delaminate in aqueous solutions. This new method of membrane fabrication offers a practical model for making channel-based biomimetic membranes, which may lead to technological applications in reverse osmosis, nanofiltration, and ultrafiltration membranes.

Introduction

Membranes are an energy efficient method for separations. ADDIN EN.CITE [1-3] Compared to conventional separation methods such as distillation, extraction, and crystallization; membrane separations require much lower energy consumption and offer high separation efficiency.[3] The ideal membrane should be able to selectively transport target molecules at high rates while excluding non-target molecules at high efficiency, i.e. membranes should have a combination of high permeability and high selectivity. However, current membrane materials exhibit a permeability selectivity trade-off; high permeability membranes have lower selectivity. This trade-off does not apply to natural membranes,[4] which has led to a considerable interest in pursuing bioinspired and biomimetic membrane materials.

A key class of functional elements for transport in biological membranes are channel proteins . Billions of years of evolution have resulted in protein channels with the ability to mediate transportation of specific targets such as ions and water in a highly efficient manner. To replicate their high selectivity and efficiency, a variety of intricate artificial transmembrane transport systems have been developed using synthetic methods. ADDIN EN.CITE [5-9] In addition to their possible applications in therapeutic treatment[10, 11] and sensing techniques,[12, 13] artificial transport systems demonstrate great potential for separations applications if they can be fabricated into stable scalable membranes. The advantages of using synthetic channels rather than natural proteins include lower cost, higher stability, and better chemical resistance. ADDIN EN.CITE [14-17]

Natural lipid-based biological membranes, although allowing for increased insertion of either natural or synthetic transmembrane proteins, have poor mechanical properties, which limits their use in commercial applications.[18] Robust materials from self-assembled block copolymers are ideal candidates to simulate the structure and environment of lipid bilayers, ADDIN EN.CITE [19-21] while providing higher stability for specific applications. Similar to natural amphiphiles like lipid molecules, amphiphilic block copolymers can form well-defined self-assembled structures (vesicle, worm-like micelles, and spherical micelles). By tuning the volume fractions of the blocks, the number of repeat units, and the incompatibility between blocks, a variety of self-assembled structures can be constructed both in solution and bulk phase.[21, 22] In particular, the self-assembly of amphiphilic diblock copolymers in aqueous solutions has been extensively studied in theoretical ADDIN EN.CITE [23-25] and experimental work, ADDIN EN.CITE [26-28] demonstrating the high potential of block copolymers for building biomimetic membrane materials.

Here, we demonstrate procedures to create stable membranes using self-assembled block copolymer lamellar structures, which could be ideal for either natural or synthetic channel incorporation. Such a design has several advantages. Firstly, the self-assembled lamellar structure resembles the bilayer structure of lipid membranes with alternating hydrophobic and hydrophilic blocks, which can maintain the orientation and function of channel molecules. Secondly, by controlling the number of the layers of lamellae, the thickness of the membrane can be tuned. This tuning is beneficial for finding the balance between separation effectiveness and mechanical properties of the membranes. Finally, the rich choices and functionality available from the large varieties of polymers possible offer more opportunities for fabricating membranes for desired purposes or post-functionalization.

To demonstrate the feasibility of this lamellar membrane design, a triblock copolymer, poly(isoprene)-*block*-poly(ethylene oxide)-*block*-poly(isoprene) (PI-PEO-PI) was chosen to fabricate membranes (Figure 1). Multiblock copolymers like ABA triblock copolymers have been previously explored for vesicle self-assembly, ADDIN EN.CITE [29-34] membrane fabrication[35, 36] and channel protein insertions[37], but the work described within this paper uses the hydrophilic PEO block as the mid-block, which differentiates our system from the previously reported works. The PI-PEO-PI triblock copolymer was chosen for two reasons. First, it is possible to chemically cross-link the hydrophobic PI domains using UV-triggered thiol-ene click chemistry[38] after fabrication of the lamellar structure. Furthermore, the PEO mid-block connecting the two PI blocks serves as a permeable intermediate bridging layer, which will act as a physical cross-link, maintaining the connection between the hydrophobic domains when the membrane swells in water . The nanoscale structure of the self-assembled membrane was characterized using small-angle X-ray scattering (SAXS), atomic force microscopy (AFM), and Fourier-transform infrared spectroscopy (FTIR). We envision that by self-assembling PI-PEO-PI layers followed by UV-mediated thiol-ene cross-linking will lead to the formation of robust and stable membranes with well-defined nanostructures. Such a material will be highly desirable in future assembly of functional artificial channel-based biomimetic membranes.

Experimental

General

All commercial chemicals in this study were used as received unless stated otherwise. All solvents in this study were extra dry. The nuclear magnetic resonance (NMR) experiments were performed on an Avance AV3HD 500 NMR spectrometer (Bruker) at room temperature. All the obtained spectra were calibrated according to the residual solvent peak. The size-exclusion chromatography

(SEC) experiments were performed on an EcoSEC HLC-8320GPC (Tosoh Bioscience) equipped with a DAWN 8^+ multi-angle static light scattering detector (Wyatt Technology). The Fourier transform infrared (FTIR) measurements were performed using a Vertex 70 spectrometer equipped with a liquid nitrogen cooled broad band mercury cadmium telluride(MCT) detector. All measurements were made under constant nitrogen purge on a Veemax variable angle Attenuated total reflection (ATR) accessory (Pike Technology) at an incident angle of 60° with a Germanium ATR crystal and spectra collected as an average of 500 scans at 4 cm^{-1} resolution.

Synthesis of poly(isoprene) (PI)

Block copolymers containing PEO blocks were synthesized via a sequential anionic polymerization method, which is described in previous work[39]. Purified isoprene monomer (24.6 g) was slowly added to a glass reactor flask containing 500 mL column purified cyclohexane and *sec*-butyllithium (1.4 M, 7.5 mL) under an argon atmosphere. The reaction was run at 45 °C for 3 hours. Then 10-times molar excess of purified ethylene oxide was added to the reactor, and reacted for 18 h to end-functionalize the living PI chain ends. The terminal alkoxide was finally quenched with 10 mL of degassed methanol. The reaction solvent (cyclohexane) was evaporated, and the polymer was extracted with chloroform and purified with water three times. The polymer was then dried under vacuum for 24 h to afford a clear viscous liquid.

Synthesis of poly(isoprene)-*block*-poly(ethylene oxide) (PI-PEO)

PI (2.33 g) was added to a reactor flask and vacuum dried overnight to remove any residual solvent. Column purified tetrahydrofuran (THF, 500 mL) was then added to the reactor. The temperature of the reaction solution was increased to 45 °C. Freshly made potassium naphthylanide was added to the reactor by slow titration until a light green color remained in the solution for 0.5 h indicating formation of PI alkoxide chain ends. Purified ethylene oxide (3 g) was added to the reactor under a positive pressure of 2.5 psi. The reaction was allowed to react for 24 h before quenching with degassed methanol (10 mL). The reaction solvent (THF) was evaporated, and the polymer was re-dissolved in chloroform. Then the polymer solution was washed two times with water and one time with saturated NaCl solution. After, the polymer solution was dried with anhydrous Na_2SO_4 and concentrated by rotary evaporation, the polymer was then precipitated in cold acetone and finally freeze-dried in benzene to afford light yellow solid.

Synthesis of poly(isoprene)-*block*-poly(ethylene oxide)-*block*-poly(isoprene) (PI-PEO-PI)

PI-PEO (1 g) was dissolved in 50 mL THF and titrated with potassium naphthylanide. Then 0.5 equivalent of α,α'-dibromo-p-xylene dissolved in THF was added to the reaction and allowed to react for 24 h. After evaporation of the solvent, the polymer was dissolved in chloroform and washed with water twice, saturated NaCl solution once and dried with anhydrous Na_2SO_4 followed by solvent evaporation. The polymer was then precipitated in cold acetone and freeze-dried in benzene to afford a light yellow solid.

Differential Scanning Calorimetry (DSC)

The thermal properties of the polymers were determined using a Thermal Analysis Q2000 DSC under argon atmosphere. To prepare samples, polymers were loaded into hermetic aluminum pans and pressed. The samples were tested as follows: (1) equilibrate the sample at 25.0 °C, (2) heat to 100 °C (10.0 °C/min) and equilibrate for 5.0 min, (3) ramp to 25.0 °C (10.0 °C/min) and equilibrate for 5.0 min, (4) ramp to 100 °C (10.0 °C/min) and equilibrate for 5.0 min, and (5) ramp to 25.0 °C (10.0 °C/min).

Membrane fabrication

To assemble the membrane matrix, the polymer PI-PEO-PI was dissolved in toluene at defined concentrations with 1% photo initiator (diphenyl(2,4,6-trimethylbenzoyl) phosphine oxide (TMDPO)) and 4% cross-linker (pentaerythritol tetra(3-mercaptopropionate)). The solution was stirred for 12 h followed by filtration (PTFE, 0.20 μm) to remove dust before use. Silicon substrates (Process Specialties Inc., CA) were thoroughly washed with acetone, THF, and ethanol, respectively, and finally dried with N_2. Before spin coating, the cleaned substrates were pretreated with UV-ozone (UVO-Cleaner®, Jelight Company Inc., CA) for 15 min. Then a poly(3,4-ethylenedioxythiophene) polystyrene sulfonate (PEDOT:PSS) solution (Clevios™ P, Heraeus,

Germany) was spin coated on a silicon substrate at 4000 rpm for 1 min as a sacrificial layer. Finally, the polymer solution was spin coated on top of the sacrificial layer at 1000 rpm. The resulting film was annealed in toluene vapor for 45 min and then exposed to a UV light (365 nm) for 45 min in order to crosslink the film. Then the substrate was gently immersed in purified water to allow the PEDOT:PSS layer to be dissolved. The free-standing membrane was then used for further studies.

Small-angle X-ray scattering (SAXS)

The X-ray scattering study was performed using a Cu K-α sourced Xeuss 2.0 beamline (XENOCS) installed with a Dectris Pilatus 200K detector and collimation optics. The scattering wavevector, *q*, was calibrated by using a standard sample of silver behenate. The PI-PEO-PI samples for transmission SAXS experiments were prepared in a quartz capillary (1.5 mm thickness, Charles Supper Company) and annealed at 180 °C under vacuum overnight. The X-ray wavelength was 0. 9758 Å and a beam energy of 12.7 keV. All samples were tested under vacuum.

Atomic force microscopy (AFM)

The atomic force microscopy measurements were performed on a Dimension Icon (Bruker) AFM microscope using PeakForce Tapping mode. Triangular-shaped ScanAsyst-Air tip with a tip radius of 2 – 12 nm was used in this study. The laser alignment was performed by tuning the sum value to a maximum. During the measurement, the peak force setpoint was set to 500.0 pN. For collecting a typical image, the scan was performed at a scan rate of 0.977 Hz and 512 sample/line. The accuracy of the image was confirmed by checking the trace and retrace peak force curve and comparing the AFM data from trace and retrace channels. Retrace images were showed in the paper.

Results and discussion

Polymer characterization and self-assembly

The successful synthesis of the PI homopolymer, PI-PEO diblock copolymer, and PI-PEO-PI triblock copolymer was confirmed by size-exclusion chromatography (SEC) (Figure 2). As seen in Figure 2, the three SEC traces exhibit both monomodal and narrow molecular weight distributions . Both PI-PEO and PI-PEO-PI elute at shorter retention times with respect to PI, indicating both an increase in the molecular weight, and successful additions of the second PEO block and coupling of the PI-PEO diblocks to result in the PI-PEO-PI triblock copolymer. The number-average molecular weight (M_n) and polymer dispersity indexes ($Đ$) of the three polymers were calculated using ^{1}H NMR and SEC, respectively (Table 1). The volume fraction of PEO (f_{PEO}) for PI-PEO and PI-PEO-PI was determined to be 44%, which is in the volume fraction range needed for building bulk self-assembled lamellar structures with block copolymers. ADDIN EN.CITE [21, 40, 41]

The self-assembly behaviors of the block polymers PI-PEO and PI-PEO-PI were studied in the bulk phase using transmission SAXS (Figure 3). The samples were examined at 110 °C and 25 °C. At 110 °C, above the crystallization temperature of the PEO block (Figure 4), both PI-PEO and PI-PEO-PI showed three distinct peaks corresponding to lamellar structures (where q/q* = 1,√4,√9). Noticeably, the calculated domain spacing, *d* (= 2π/*q**), using SAXS (Figure 3a) for the PI-PEO-PI (11.8 nm) indicates a slight increase in *d* as compared to the PI-PEO diblock copolymer (11.6 nm). The slight increase in *d* for the triblock copolymer as compared to the PI-PEO diblock copolymer is likely due to an increase in the segregation strength with increasing M_n, which leads to larger chain stretching within the lamellae, as has been previously reported in similar multiblock copolymer systems.[42, 43]

The self-assembled structures for PI-PEO and PI-PEO-PI were then determined at room temperature (25 °C) (Figure 3b). The SAXS patterns for both the diblock and triblock copolymer indicate that a lamellar morphology persists below the crystallization temperature of the PEO block (where q/q* = 1,√4,√9,√16). Again, similar to the SAXS patterns at 110 °C, there is a slight increase in *d* for the PI-PEO-PI (16.1 nm) as compared to the PI-PEO diblock copolymer (15.0 nm). The increase in *d* at lower temperatures is due to the higher segregation strength, which is consistent with previous studies.[42] Noticeably, the SAXS pattern of PI-PEO-PI showed increased scattering intensity at low *q* range. We attribute this result to a higher crystallinity percentage of

PEO in PI-PEO compared with PI-PEO-PI.[44] Unlike covalently connected PI-PEO-PI, the PEO chains in the diblock polymer PI-PEO can move more freely and are more likely to form crystalline microregions, and be less kinetically limited when $T < T_m$. Additionally, the PEO mid-block in the PI-PEO-PI block is significantly restricted in chain movement influencing the crystallization kinetics, which has been previously reported in multiblock copolymer systems.[45] To confirm this, the melting behavior of PEO block in PI-PEO and PI-PEO-PI were studied using DSC (Figure 4). It was found that the T_m values of PI-PEO and PI-PEO-PI are close to each other (50.6 °C and 50.3 °C, respectively). However, the heat of fusion (H_m) of PI-PEO (76.4 J/g) is larger than PI-PEO-PI (68.1 J/g). The fraction of crystalized PEO block (Φ_{PEO}) can be calculated according to the equation

where is the heat of fusion for infinite PEO crystals which is 203 J/g.[46] w_{PEO} is the weight fraction of PEO in the block copolymers, which is 51.5% for both polymers. Thus, the crystallinity percentage of the PEO block in PI-PEO and PI-PEO-PI to calculated to be 73.1% and 65.1% respectively, indicating that there is indeed a larger percentage of crystallinity in PI-PEO than PI-PEO-PI.

Membrane fabrication and characterization

After confirming that the triblock copolymer PI-PEO-PI can self-assemble into a lamellar phase, we continued to look into the membrane fabrication process with spin coating. The key consideration for this membrane fabrication process is to have the self-assembled polymeric lamellar structures stacked parallel to the surface. To realize this goal, a sacrificial layer of PEDOT:PSS was first spin coated on UV-Ozone processed silicon substrates to offer a hydrophilic surface. Thus, when the lamellar starts to form on top the substrate, the PEO layer will contact the surface first due to a strong preferential interaction with the interface, favoring the parallel lamellar alignment (Figure 5). Preferential wetting of a specific polymer block to a substrate is a common method to dictate the ordering in block polymer thin films. {Hu, 2014, Directed self-assembly of block copolymers: a tutorial review of strategies for enabling nanotechnology with soft matter}[47]

The parallel lamellar alignment to the substrate surface was confirmed using AFM (Figure 6). By varying the concentration of the spin coating polymer solution and spin coating speed, membranes of different thicknesses and surface coverage were obtained. At a spin coating speed of 7000 rpm with 2 mg/mL PI-PEO-PI toluene solution, there is only one incomplete layer observed on the substrate (Figure 6a). As shown in Figure 6, the lamellar layer only covers less than a half of the surface and the shape of the formed layer is reminiscent of preferential growth in certain areas, which may indicate that the PEO crystallinity is significantly influencing the PI-PEO -PI self-assembly process on the substrate. By measuring the vertical distance between the substrate surface and the layer, a uniform step height of about 8 nm through the surface was obtained. This height is half of the domain spacing value of the PI-PEO-PI lamellar measured with SAXS at room temperature (16.1 nm). Such an observation indicates that at lower surface coverage, the triblock copolymer will bend to form a half layer on the surface. At decreased spin coating speed of 1000 rpm with the same polymer solution, both a 15 nm and a 24 nm layer are observed, which we attribute to a full "one layer" of the PI-PEO-PI polymer and "one and a half layer", respectively. The surface coverage also increased as the membrane thickness grows. By increasing the concentration of the polymer solution to 5 mg/mL and after spin coating at 2000 rpm, the "second layer" of a height of about 16 nm is clearly observed on top the first layer. The substrate surface is almost fully covered. Thus, it is concluded that by using spin coating, the polymer can form a lamellar structure that is similar to the morphology seen in the bulk phase. The lamellae are stacked parallel to the substrate surface due to a preferential interaction between the hydrophilic surface and the PEO block.[48] By controlling the concentration of the polymer solution and the spin coating speed, the thickness of the membrane can be well controlled, while maintaining the same d spacing. From the AFM, it can also be seen that there are defect regions, which are not covered by the membrane. A possible cause of this is the crystallization interference of the PEO block to the block copolymer self-assembly process.

Once the self-assembled membrane possessing the parallel-stacked lamellar structure was constructed, as confirmed by AFM, the in-situ cross-linking of the membrane was performed

through thiol-ene chemistry for further fabrication of free-standing membranes. After spin coating the solution containing the polymer, thiol cross-linker, and UV photo-initiator, the membrane was irradiated under UV 365 nm for different periods of time. FTIR spectra were collected of the membrane to determine the best UV duration time. As shown in Figure 7, the FTIR absorbance peak around 1650 cm^{-1} corresponds to the vinyl groups of the PI block.[48] As the UV irradiation duration time increases, the peak decreases within 45 min. The peak remained the same for longer time indicating a 45 min duration of UV irradiation time is sufficient for cross-linking.

To obtain a free standing thin membrane, a sacrificial layer was used.[49] After substrate processing, a water-soluble polymer layer of PEDOT:PSS was first formed on the substrate through spin coating. Then the PI-PEO-PI layer was spin coated on top and cross-linked in situ. Afterwards, the film was slowly immersed into water to dissolve the sacrificial layer, which results in a thin membrane located on the water surface. As shown in Figure 8a, the AFM image of the spin coated PEDOT:PSS indicates that the layer is flat. Then the PI-PEO-PI polymer solution with a concentration of 20 mg/mL was spin coated at 1000 rpm on top of the sacrificial PEDOT:PSS layer forming lamellar structures. The substrate was then immersed in water and the transparent free-standing membrane of PI-PEO-PI was successfully obtained (Figure 8c). We hypothesize that the PI-PEO-PI membrane is able to be swollen with water without breaking up due to the physical cross-linking of the PI domains by the "bridging" PEO chains. In ABA type triblock copolymer systems like PI-PEO-PI that self-assemble into lamellar morphologies, roughly 60% of the mid-block chains are predicted to be "looping".[50] That is, the A-blocks will reside in the same domain, which results in the B mid-block bending to form a loop. Although only a fraction of the PEO mid-blocks are "bridging" in our system, there are enough physical cross-links to prevent the membrane from delaminating. Ideally, if one is trying to maximize the membrane stability in water and increase the mechanical properties, all B mid-block chains will be "bridging". Future directions in the area of block polymer-based membranes will have to consider polymer chain architecture with respect to performance and long-term stability.

Conclusions

In this work, we demonstrate the feasibility of using triblock copolymer self-assembled lamellar films to fabricate a membrane matrix that simulates the natural lipid bilayer membrane. The stacked lamellae parallel to the substrate are appropriate for artificial channel insertion. By using sequential anionic polymerization and diblock copolymer coupling, the triblock copolymer PI-PEO-PI was synthesized with a narrow molecular weight distribution. The bulk self-assembled lamellar morphology of the triblock copolymer was confirmed by transmission SAXS. A membrane was fabricated with the triblock copolymer through spin coating and studied with AFM . It was found that by using a silicon wafer substrate surface that the PEO preferentially wets, self-assembled parallel-oriented lamellar structures can be obtained. We hypothesize that the challenges encountered with non-uniformity of the spin-coated films were related to the crystallinity of the PEO block. Future work should try to mitigate the crystallinity effects to allow for more uniform film formation. Finally, by means of a sacrificial layer, in situ UV chemical cross-linking, and physical cross-linking from the polymer architecture, free standing floating membrane layers were fabricated. Inspired by the promising results of this work, further studies of channel incorporation into the lamellar membrane matrix is underway in our labs for filtration experiments.

Acknowledgements

The authors acknowledge financial support from the National Science Foundation CAREER grant (CBET-1552571) to MK for this work. Support was also provided through CBET-1705278 and DMR- 1709522 for various aspects of this work.

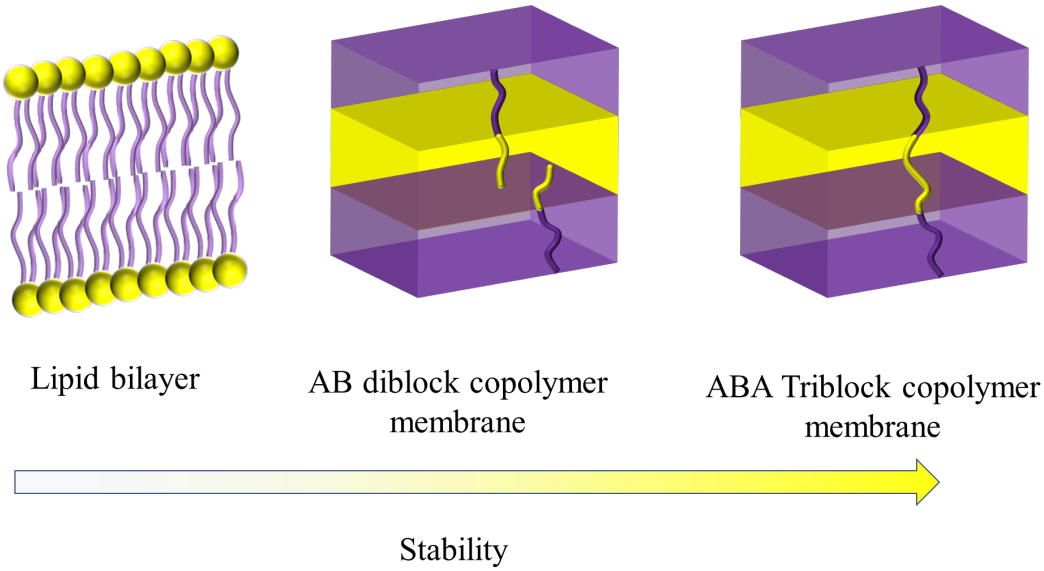

Figure 1. Schematic representation of the self-assembled lamellar structures using lipids, block copolymers, and triblock copolymers. The membrane stability is found to increase with increasing molecular architecture complexity.

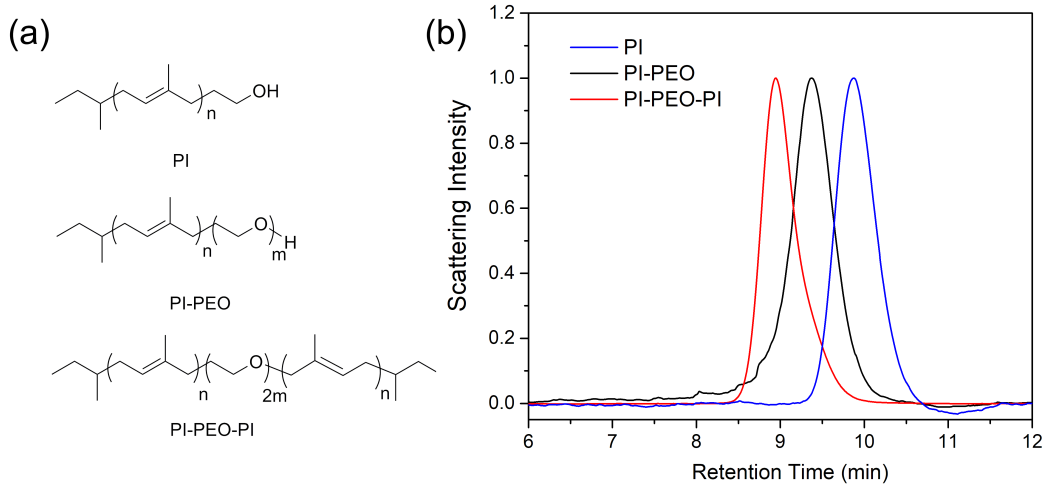

Figure 2. (a) Chemical structures of PI, PI-PEO and PI-PEO-PI (b) Size-exclusion chromatography (SEC) traces using a multi-angle light scattering detector for PI, PI-PEO, and PI-PEO-PI. The SEC traces confirm that the homopolymer, diblock copolymer, and triblock copolymer were successfully synthesized.

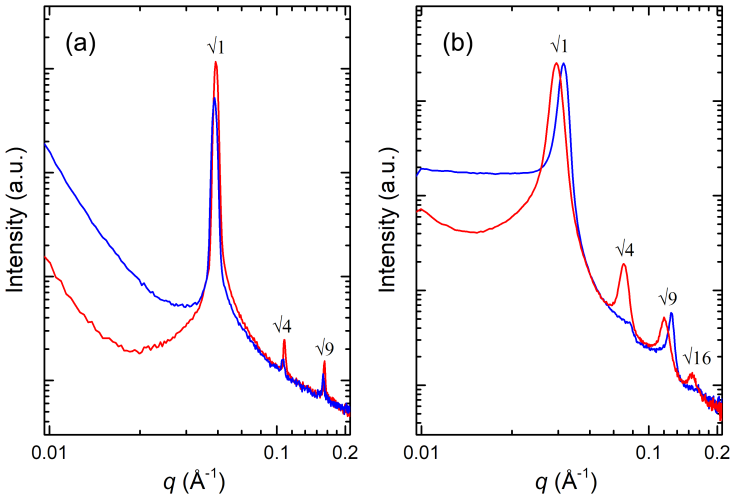

Figure 3. Isothermal transmission SAXS patterns for PI-PEO (blue) and PI-PEO-PI (red) obtained at 110 °C (a) and 25 °C (b). Both polymer samples at 110 °C and 25 °C exhibit a lamellar morphology.

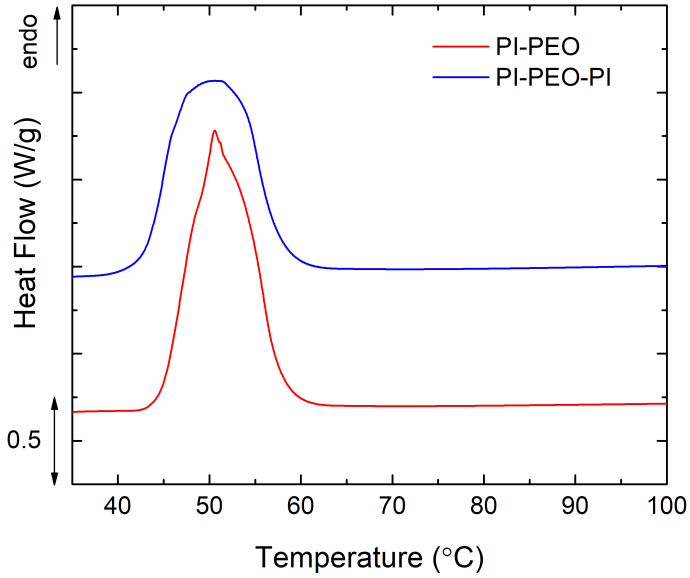

Figure 4. DSC traces of PI-PEO and PI-PEO-PI from second heating ramp results at 10 °C/min. The T_m of PI-PEO and PI-PEO-PI is determined to be 50.6 °C and 50.3 °C respectively. The heat of fusion H_m of PI-PEO and PI-PEO-PI is calculated to be 76.4 J/g and 68.1 J/g respectively.

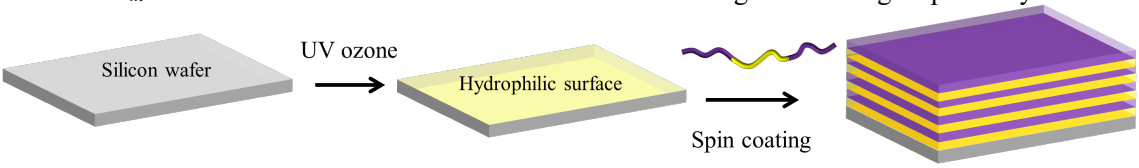

Figure 5. Schematic representation of the fabrication process of parallel stacked PI-PEO-PI lamellar membrane.

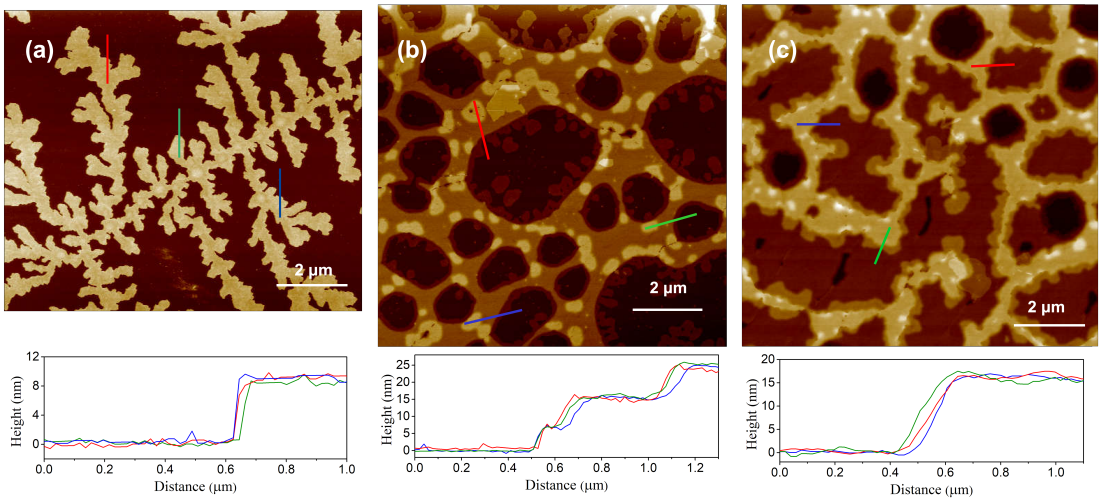

Figure 6. AFM images showing the surface morphology of thin films spin coated with toluene solution of PI-PEO-PI at different speeds, and the step height of the lamellar structures. (a) 2 mg/mL toluene solution of PI-PEO-PI spin coated at 7000 rpm for 1 min (b) 2 mg/mL toluene solution of PI-PEO-PI spin coated at 1000 rpm for 1 min (c) 5 mg/mL toluene solution of PI-PEO-PI spin coated at 2000 rpm for 1 min. The defect areas on the membrane are likely due to the crystallization of the PEO interrupting the self-assembly process.

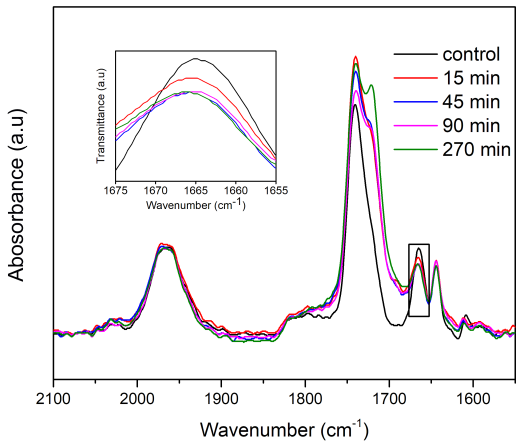

Figure 7. FTIR absorption spectra of PI-PEO-PI cross-linked under UV 365 nm for different durations of time. The peak at 1650 cm^{-1} corresponds to the vinyl groups in the PI block. The decrease of the peak as UV time increases indicates successful cross-linking.

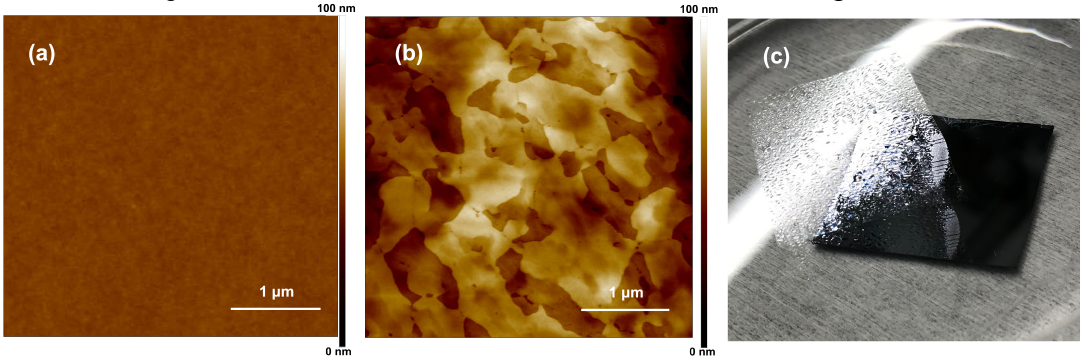

Figure 8. (a) AFM image of the surface morphology of the sacrificial PEDOT:PSS polymer layer. (b) AFM image of the surface morphology of the lamellar structured PI-PEO-PI membrane. (c) PI -PEO-PI lamellar membrane after on the water surface after removing from the substrate.

Table 1. Molecular weight, volume ratio of the polymers and domain spacing values of the self-assembled lamellar structures reported in this work.

[a] Number-average molecular weight of the polymers was determined from ^{1}H NMR spectroscopy. [b] Dispersity index (*Mw*/*Mn*) was determined from size exclusion chromatography (SEC). [c] Volume ratio of the block copolymer was calculated using ^{1}H NMR data. We use the density of PI as 0.906 g/mL and the density of PEO as 1.207 g/mL at 25 °C. [d, e] Domain spacing values of the lamellar structures at 110 °C and 25 °C were calculated from SAXS experiments performed at the reported temperatures.

References

ADDIN EN.REFLIST 1. P. Marchetti, M. F. Jimenez Solomon, G. Szekely and A. G. Livingston, *Chemical Reviews*, 2014, **114**, 10735-10806.

2. P. Bernardo, E. Drioli and G. Golemme, *Industrial & Engineering Chemistry Research*, 2009, **48**, 4638-4663.
3. M. T. Ravanchi, T. Kaghazchi and A. Kargari, *Desalination*, 2009, **235**, 199-244.
4. H. B. Park, J. Kamcev, L. M. Robeson, M. Elimelech and B. D. Freeman, *Science*, 2017, **356**, eaab0530.
5. M. Barboiu, *Angewandte Chemie International Edition*, 2012, **51**, 11674-11676.
6. B. Gong and Z. Shao, *Accounts of chemical research*, 2013, **46**, 2856-2866.
7. S. Matile, A. V. Jentzsch, J. Montenegro and A. Fin, *Chemical Society Reviews*, 2011, **40**, 2453-2474.
8. L. Chao, X. Deng, W. Wang, S. Qi, X. Zhang, C. Zhang, F. Yang, B. Yang, Z. Dong and J. Liu, *Angewandte Chemie*, 2017.
9. S. Howorka, *Nature nanotechnology*, 2017, **12**, 619.
10. M. Zhang, P. P. Zhu, P. Xin, W. Si, Z. T. Li and J. L. Hou, *Angewandte Chemie*, 2017, **129**, 3045-3049.
11. A. G. Cioffi, J. Hou, A. S. Grillo, K. A. Diaz and M. D. Burke, *Journal of the American Chemical Society*, 2015, **137**, 10096-10099.
12. J. R. Burns, A. Seifert, N. Fertig and S. Howorka, *Nature nanotechnology*, 2016, **11**, 152.
13. C. Lang, X. Zhang, Z. Dong, Q. Luo, S. Qiao, Z. Huang, X. Fan, J. Xu and J. Liu, *Nanoscale*, 2016, **8**, 2960-2966.
14. R. H. Tunuguntla, R. Y. Henley, Y.-C. Yao, T. A. Pham, M. Wanunu and A. Noy, *Science*, 2017, **357**, 792-796.
15. C. Lang, W. Li, Z. Dong, X. Zhang, F. Yang, B. Yang, X. Deng, C. Zhang, J. Xu and J. Liu, *Angewandte Chemie International Edition*, 2016, **55**, 9723-9727.
16. Y.-x. Shen, W. Si, M. Erbakan, K. Decker, R. De Zorzi, P. O. Saboe, Y. J. Kang, S. Majd, P. J . Butler and T. Walz, *Proceedings of the National Academy of Sciences*, 2015, **112**, 9810-9815 .
17. T. M. Fyles, *Chemical Society Reviews*, 2007, **36**, 335-347.
18. L. Rilfors, G. Lindblom, Å. Wieslander and A. Christiansson, in *Membrane Fluidity*, Springer, 1984, pp. 205-245.
19. B. M. Discher, Y.-Y. Won, D. S. Ege, J. C. Lee, F. S. Bates, D. E. Discher and D. A. Hammer , *Science*, 1999, **284**, 1143-1146.
20. D. E. Discher and A. Eisenberg, *Science*, 2002, **297**, 967-973.
21. Y. Mai and A. Eisenberg, *Chemical Society Reviews*, 2012, **41**, 5969-5985.
22. F. S. Bates and G. Fredrickson, *Physics today*, 2000.
23. B. M. Discher, H. Bermudez, D. A. Hammer, D. E. Discher, Y.-Y. Won and F. S. Bates, *The Journal of Physical Chemistry B*, 2002, **106**, 2848-2854.
24. H. Bermudez, A. K. Brannan, D. A. Hammer, F. S. Bates and D. E. Discher, *Macromolecules*, 2002, **35**, 8203-8208.
25. J. C.-M. Lee, M. Santore, F. S. Bates and D. E. Discher, *Macromolecules*, 2002, **35**, 323-326.
26. R. J. Hickey, A. S. Haynes, J. M. Kikkawa and S.-J. Park, *Journal of the American Chemical Society*, 2011, **133**, 1517-1525.
27. D. M. Vriezema, P. M. Garcia, N. Sancho Oltra, N. S. Hatzakis, S. M. Kuiper, R. J. Nolte, A. E. Rowan and J. van Hest, *Angewandte Chemie*, 2007, **119**, 7522-7526.

28. D. A. Christian, S. Cai, D. M. Bowen, Y. Kim, J. D. Pajerowski and D. E. Discher, *European Journal of Pharmaceutics and Biopharmaceutics*, 2009, **71**, 463-474.
29. C. Nardin, T. Hirt, J. Leukel and W. Meier, *Langmuir*, 2000, **16**, 1035-1041.
30. T. Hayashi, K. Takeshima and A. Nakajima, *Polymer journal*, 1985, **17**, 1273.
31. R. Yoda, S. Komatsuzaki, E. Nakanishi, H. Kawaguchi and T. Hayashi, *Biomaterials*, 1994, **15**, 944-949.
32. H. P. Maassen, J. Yang and G. Wegner, 1990.
33. J. Noolandi, A.-C. Shi and P. Linse, *Macromolecules*, 1996, **29**, 5907-5919.
34. Z. Zhou and B. Chu, *Macromolecules*, 1988, **21**, 2548-2554.
35. C. Nardin, M. Winterhalter and W. Meier, *Langmuir*, 2000, **16**, 7708-7712.
36. A. González-Pérez, V. Castelletto, I. W. Hamley and P. Taboada, *Soft Matter*, 2011, **7**, 1129-1138.
37. W. Meier, C. Nardin and M. Winterhalter, *Angewandte Chemie International Edition*, 2000, **39**, 4599-4602.
38. C. E. Hoyle and C. N. Bowman, *Angewandte Chemie International Edition*, 2010, **49**, 1540-1573.
39. M. A. Hillmyer and F. S. Bates, *Macromolecules*, 1996, **29**, 6994-7002.
40. F. S. Bates and G. H. Fredrickson, *Annual review of physical chemistry*, 1990, **41**, 525-557.
41. M. Templin, A. Franck, A. Du Chesne, H. Leist, Y. Zhang, R. Ulrich, V. Schädler and U. Wiesner, *Science*, 1997, **278**, 1795-1798.
42. L. Wu, E. W. Cochran, T. P. Lodge and F. S. Bates, *Macromolecules*, 2004, **37**, 3360-3368.
43. S.-M. Mai, W. Mingvanish, S. C. Turner, C. Chaibundit, J. P. A. Fairclough, F. Heatley, M. W . Matsen, A. J. Ryan and C. Booth, *Macromolecules*, 2000, **33**, 5124-5130.
44. I. W. Hamley, J. P. A. Fairclough, N. J. Terrill, A. J. Ryan, P. M. Lipic, F. S. Bates and E. Towns-Andrews, *Macromolecules*, 1996, **29**, 8835-8843.
45. T. R. Panthani and F. S. Bates, *Macromolecules*, 2015, **48**, 4529-4540.
46. Z. Qiu, T. Ikehara and T. Nishi, *Polymer*, 2003, **44**, 2799-2806.
47. H. Hu, M. Gopinadhan and C. O. Osuji, *Soft matter*, 2014, **10**, 3867-3889.
48. M. Kalloudis, E. Glynos, S. Pispas, J. Walker and V. Koutsos, *Langmuir*, 2013, **29**, 2339-2349.
49. W. Cheng, M. J. Campolongo, S. J. Tan and D. Luo, *Nano Today*, 2009, **4**, 482-493.
50. M. W. Matsen and R. Thompson, *The Journal of chemical physics*, 1999, **111**, 7139-7146.